Earthquakes and Structures, *Vol. 10, No. 4 (2016) 829-847*
DOI: http://dx.doi.org/10.12989/eas.2016.10.4.829

Seismic base isolation for structures using river sand

S.J. Patil[*1], G.R. Reddy[2a], R. Shivshankar[3b], Ramesh Babu[4c], B.R. Jayalekshmi[3b] and Binu Kumar[2c]

[1]*Heavy Water Board, Mumbai, India*
[2]*BARC & HBNI, Mumbai, India*
[3]*NITK, Suratkal, India*
[4]*CPRI, Banglore, India*

(Received July 10, 2012, Revised April 9, 2015, Accepted February 8, 2016)

Abstract. Generally seismic isolation is achieved by supporting the structure on laminated rubber bearings, friction pendulum bearings, roller bearings etc. Very little work has been performed using soil as a base isolation media. Experiments and analytical work has been performed on a structural model with isolated footing and found encouraging results. Details of this work are presented in this paper.

Keywords: isolated footings; natural seismic base isolation; modulus reduction; IS 1893

1. Introduction

In a traditional seismic design approach, strength of the structure is suitably adjusted to resist the earthquake forces. In base isolation technique approach, the structure is essentially decoupled from earthquake ground motions by providing separate isolation devices between the base of the structure and its foundation. The main purpose of the base isolation device is to attenuate the horizontal acceleration transmitted to the superstructure.

All the base isolation systems have certain features in common. They have flexibility and energy absorbing capacity. The main concept of base isolation is to shift the fundamental period of the structure out of the range of dominant earthquake energy frequencies and increasing the energy absorbing capability. The concept is explained in Fig. 1. Presently base isolation techniques are mainly categorized into three types viz. Passive base isolation techniques, Hybrid isolation with semi-active devices and Hybrid base isolation with passive energy dissipaters.

Passive base isolation techniques have been used in the past. Laminated rubber bearings (LRB) (Jangid and Datta 1992), which are made of thin layers of steel plates and rubber built in layers one over the other, have horizontal flexibility, high vertical stiffness and they can be characterized by natural frequency and damping constant.

*Corresponding author, Scientific Officer, E-mail: sjp_patil@yahoo.co.in
[a]Outstanding Scientist and Professor
[b]Professor
[c]Scientific Officer

http://www.techno-press.com/journals/eas&subpage=7 ISSN: 2092-7614 (Print), 2092-7622 (Online)

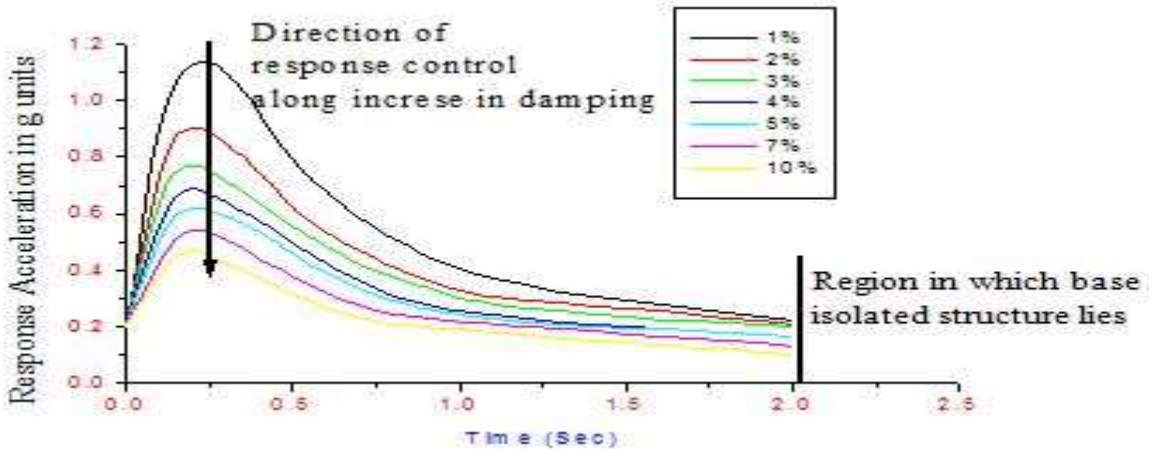

Fig. 1 Concepts of base isolation and dampers

New Zealand bearing system (Naeim and Kelly 1999), invented in New Zealand in the year 1975, is improved version of laminated rubber bearing wherein a centrally located lead core is introduced, which has energy dissipating capacity. The presence of lead core reduces displacement of the isolator and isolator essentially works as hysteretic damper device. The device has been extensively used in New Zealand, Japan and USA (Ivan *et al*. 1996). Buildings isolated with these devices performed well during the 1994 North ridge earthquake and 1995 Kobe earthquake.

Resilient-Friction Base Isolation (R-FBI) system proposed by Mostaghel and Khodaverdian consists of concentric layers of Teflon coated plates which will have sliding resistance and a central core of rubber, which will have beneficial effect of resilience of a rubber.

Friction pendulum system (FPS) uses geometry and gravity to achieve the desired seismic isolation. It is based on well-known engineering principles of pendulum motion. The structure supported by the FPS responds to the earthquake motions with small pendulum motions. The friction damping absorbs the earthquake energy. There is a variety of friction pendulum systems developed; such as, variable frequency pendulum isolators, variable curvature pendulum systems, sliding concave foundation, double concave friction pendulum system, Triple friction pendulum bearing.

Hybrid isolation system with semi-active devices (Massimo *et al*. 2004) - Hybrid isolation system uses both passive isolation systems and semi active/active controlling devices. The Medical Centre of the Italian Navy at Ancona, Italy, was provided with a hybrid system composed by Low Damping Rubber Bearings (LDRBs) acting as passive seismic isolators, and Magneto-rheological (MR) dampers, acting as semi- active controlling devices.

Hybrid base isolation with passive energy dissipaters - The energy dissipating devices such as elasto-plastic dampers (Parulekar *et al*. 2007), visco-elastic dampers (Kumar *et al*. 2004), lead extrusion dampers (Parulekar *et al*. 2004), etc mainly dissipate the earthquake energy and thereby reduce the effect of the earthquake on the structure. These devices can be used at the base of the structure or in superstructure at appropriate locations. They can be used in combination with passive base isolation techniques.

Many significant advantages can be drawn from buildings provided with seismic isolation. The isolated buildings will be safe even in strong earthquakes. The response of an isolated structure

can be ½ to 1/8 of the traditional structure. Since the super structure will be subjected to lesser earthquake forces, the cost of isolated structure compared with the cost of traditional structure for the same earthquake conditions will be cheaper. The seismic isolation can be provided to new as well as existing structures. The buildings with provision of isolators can be planned as regular or irregular in their plan or elevations (Zhou *et al*. 2004).

Many of the base isolation techniques demand regular inspection and maintenance of the system. The performance of the isolators under severe fire is questionable.

As such it is desirable to develop such an isolator, which has a life span equal or more than the life of a structure, free from effects of environment and fire. Also it should be free from maintenance. In addition to promote green technology, it will be an ideal case if researchers develop an isolator using natural materials such as sand, soil.

In the past, experiments have been performed on structures resting on sand layer (Yegian and Kadakal 2004) and soil mixed with rubber (Tsang *et al*. 2012). Such systems dissipate earthquake energy before reaching to the structure and are useful for wide range of frequencies. Variety of soil is available in abundance in nature and each type of soil exhibit different properties. The same soil exhibits different properties in dry and wet conditions or static and dynamic conditions. The shear modulus in static and that in dynamic conditions varies largely. The properties of the soil can be altered by providing geo-membrane in the soil (Yegian and Kadakal 2004) or rubber (Tsang *et al*.

Fig. 2(a) Experimental setup on shake table

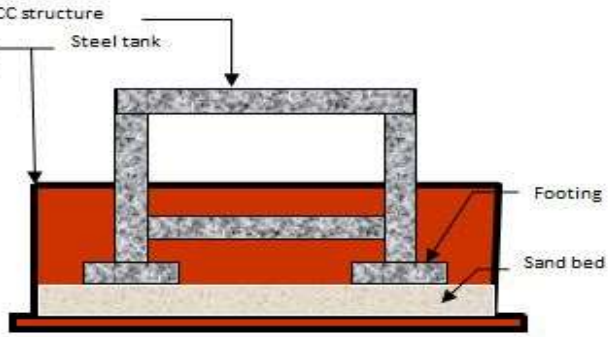

Fig. 2(b) Sketch illustrating the experimental setup

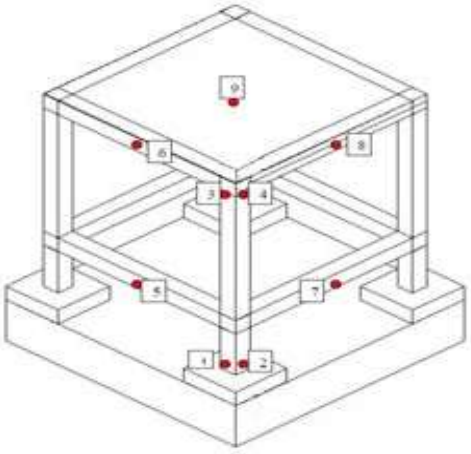

Fig. 2(c) Reinforced Cement Concrete (RCC) model with isolated footing with accelerometer locations

Table 1 River sand properties

Property	Value	Property	Value	Property	Value	Property	Value
Gravel	5.6%	Cu	7.37	Silt+Clay	4.4%	Sp.gravity	2.66
Coarse sand	19.4%	Cc	1.12	D60	1.18 mm	emax	0.77
Medium Sand	53%	γdmax	1.71 g/cc	D10	0.16 mm	emin	0.48
Fine Sand	17.6%	γdmin	1.40 g/cc	D30	0.46 mm		

2012). The soil properties can also be altered by mixing rubber (Feng and Sutter 2000, Tsang 2008, Srijit and Aniruddha 2012), shredded tires in the soil (Foose and Benson 1996, Peter and Tuncer 1994). Studies are also carried out to know the effect of 'Soil Structure Interaction (SSI) on base isolated systems and fixed base structures on soft soil (Karabork *et al*. 2014), which points out that the performance of isolator is proportional to its stiffness.

The cost of soil is meager and needs no maintenance cost. Knowing these facts, clean river sand was tried as base isolation material and experiments were conducted on a RCC frame model having isolated footing as shown in Fig. 2. River sand, having engineering properties shown in Table 1 (BRNS research report 2009) is used in the experiment.

2. Isolated footing model

Size of the model is 1.2×1.2×1.5 m and the model is provided with isolated footings of size 0.35×0.35×0.1 m thickness. The size of cross section of beams and columns is 0.1×0.1 m. and roof slab thickness is 0.05 m. A metallic box of size 2.0 m×2.0 m×1.2 m height as shown in Fig. 1(a) is used and is filled with 300 mm thick layer of the dry sand/wet sand/dry sand with geo-membrane/wet sand with geo-membrane in separate cases.

The box is fixed on tri-axial shake table and reinforced cement concrete (RCC) model is kept on the sand layer. The locations of the accelerometers fixed on the model are indicated in Fig. 2c. Different tests were conducted on the model.

3. Sine sweep tests

Natural frequencies of the model were established by conducting resonance search tests with sinusoidal motion of 0.1 g for fixed base (FXISO) model and 0.2 g for other models with a sweep rate of 1 octave per minute. Using transfer functions of output to the input, the frequencies are obtained and listed in Table 2. The values given in the bracket are analytical frequencies. It is seen that as compared to the fixed base case, the frequencies of the model on sand layer, sand layer with geo-membrane, wet sand and wet sand with geo-membrane in horizontal direction are reduced. Percentage reduction in frequencies in horizontal directions is also shown in Table 2.

Using half power method, damping ratios for the model with different base conditions were estimated from the experimental results and are given in Table 3. The ratios are compared with those of fixed base model and it is seen that for all the cases, damping ratios have increased; the increase is from 117% for IDSGM case to 262% for ISOWETG case in horizontal direction.

Table 2 Natural frequencies from sine sweep test

Sr. No	Model condition/ direction	Frequency Hz			Percentage reduction		
		X	Y	Z	X*	Y*	Z**
1	Fixed base (FXISO)	4.39 (4.58)	4.27 (4.58)	- (65.61)	-	-	-
2	Supported on a layer of dry sand (ISODRY)	3.90 (3.11/1.90)	3.58 (3.11/1.90)	11.60 (10.93/10.93)	-11.16	-16.16	- (-83.34/-83.34)
3	Supported on a layer of dry sand + geo-membrane (RDSGM)	2.82 (2.80/1.63)	2.81 (2.80/1.63)	10.69 (9.60/9.60)	-35.76	-34.19	- (-85.36/-85.36)
4	Supported on layer of saturated sand (ISOWET)	3.09 (2.76/1.24)	3.10 (2.76/1.24)	10.46 (8.52/ 8.52)	-29.61	-27.40	- (-87.01/ -87.01)
5	Wet sand + Geo-membrane (ISOWETG)	2.51 (1.49/0.96)	2.38 (1.49/0.96)	10.12 (6.97/6.97)	-42.82	-44.26	- (-89.38/-89.38)

Note: Values shown in brackets are analytical frequencies of the model obtained for zone III/zone V time histories

*The values indicate percentage reduction in frequencies with respect to fixed base case

** The values indicate percentage reduction in frequencies with respect to fixed base case analytical values

Table 3 Damping ratios estimated from resonance tests

Sr. No.	Model condition/ direction	Damping ratio			Percentage variation	
		X	Y	Z	X*	Y*
1	Fixed base (FXISO)	4.50	4.34	-		
2	Supported on a layer of dry sand (ISODRY)	12.87 (10.47/21.88)	11.76 (10.47/21.88)	9.70 -	186.00	170.96
3	Supported on a layer of dry sand + geo-membrane (IDSGM)	9.80 (9.88/23.73)	10.00 (9.88/23.73)	8.06 -	117.77	130.41
4	Supported on layer of saturated sand (ISOWET)	12.18 (10.11/26.46)	11.26 (10.11/ 26.46)	12.09 -	170.66	159.44
5	Wet sand + Geo-membrane (ISOWETG)	13.73 (22.07/28.14)	15.72 (22.07/28.14)	8.92 -	205.11	262.21

Note: Values shown in brackets are analytical damping ratios of the model obtained for zone III/zone V time histories

*The values indicate percentage increase in damping ratios with respect to fixed base case

4. Test for IS 1893 zone III design basis ground motion

Tests were conducted using artificial acceleration time histories which are compatible to the IS-1893 code - zone III design response spectrum (IS 1893, 2002) as shown in Fig. 3(a). Table 4 shows maximum accelerations recorded at different locations on the isolated footing model. From the table, it is seen that the accelerations at roof level are reduced in horizontal directions for all the cases i.e., ISODRY, IDSGM, ISOWET and ISOWETG as compared to fixed base case. The minimum reduction of 14.40% for ISOWET and maximum reduction of 35.70% for ISODRY case is seen.

Acceleration responses recorded by roof level accelerometer A3, along X direction are

compared in all the cases in Fig. 4(a) to 4(d). It is seen from the graphs that the peak accelerations recorded are less compared to the fixed base case. Fourier transform amplitudes of the A3 signal are obtained and shown in Fig. 5(a) and Fig 5(b). It can be seen that there is a reduction in the frequency in all the cases as compared to the frequency of fixed base model.

To understand the frequency contents of the acceleration signals, recorded as shown in Fig. 2 at different locations of the model, response spectrum for 5% damping was generated and is shown in

Figs. 6 to 9. It can also be clearly seen that there is a shift in the frequency in all the cases compared to the case of fixed base. Reduction in frequencies along with increase in damping resulted in reduction in accelerations along horizontal direction compared to the fixed base case as shown in Table 4. This conclusion verifies with above FFT analysis. However along vertical direction, there is a small rise in acceleration as shown in Table 4. This is due to the rigid frequency of 65.61 Hz has reduced to the zone of amplification e.g., 9.47 Hz in the case of ISODRY.

Table 4 Response accelerations (m/sec^2) on the model subjected to Time History Compatible to IS Code Zone III

Accelero-meter Location	Z3-FXISO	Z3-ISODRY		Z3-IDSGM		Z3-ISOWET		Z3-ISOWETG	
	Max acc	Max acc	% variation	Max acc	% variation	Max acc	% variation	Max acc	% variation
A3	7.06	5.21	-26.20	4.84	-31.44	5.57	-21.10	5.20	-26.35
A6	7.06	5.38	-23.80	4.66	-33.99	4.99	-29.32	5.20	-26.35
A4	7.59	4.88	-35.70	5.18	-31.75	6.14	-19.10	5.20	-31.49
A8	7.29	4.79	-34.29	5.45	-25.24	6.24	-14.40	5.30	-27.30
A9	3.59	3.77	5.01	3.64	1.39	3.67	2.23	3.90	8.64

A3=Dir-X, location-beam-column junction at Roof level; A6=Dir-X, location-at mid span of roof beam; A4=Dir-Y, location-beam-column junction at Roof level; A8=Dir-Y, location-at mid span of roof beam; A9=Dir-Z, location - center of slab. Note - Experimental accelerations are picked up after excluding spikes, which have occurred due to shake table hydraulic system

Table 5 Response accelerations (m/sec^2) on the model subjected to Time History Compatible To IS Code Zone V

Accelerometer location	Z5-FXISO	Z5-ISODRY		Z5-RDSGM		Z5-ISOWET		Z5-ISOWETG	
	Max acc	Max acc	% variation	Max acc	% variation	Max acc	% variation	Max Acc	% variation
A3	14.30	7.41	-48.18	6.72	-53.01	10.00	-30.07	9.98	-30.21
A6	14.30	7.89	-44.83	5.63	-60.63	10.50	-26.57	10.00	-30.07
A4	14.70	7.23	-50.82	7.21	-50.95	10.50	-28.57	9.77	-33.54
A8	14.70	7.70	-47.62	8.09	-44.97	11.70	-20.41	10.00	-31.97
A9	8.38	6.93	-17.30	6.73	-19.69	6.13	-26.85	7.00	-16.47

A3=Dir-X, location-beam-column junction at Roof level; A6=Dir-X, location-at mid span of roof beam; A4=Dir-Y, location-beam-column junction at Roof level; A8=Dir-Y, location-at mid span of roof beam; A9=Dir-Z, location - center of slab. Note - Experimental accelerations are picked up after excluding spikes, which have occurred due to shake table hydraulic system

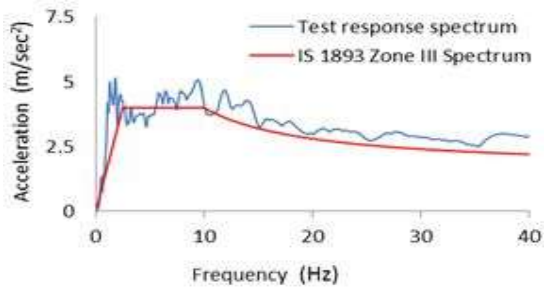

Fig. 3(a) IS 1893 zone III design response spectrum

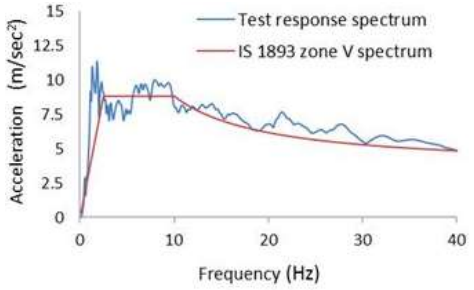

Fig. 3(b) IS 1893 zone V design response spectrum

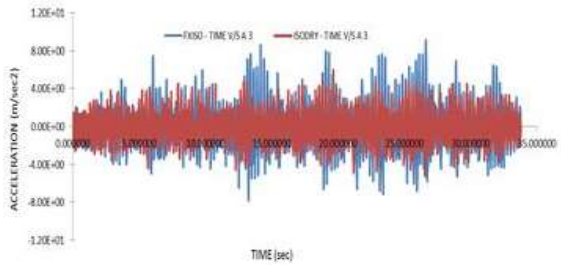

Fig. 4(a) Acceleration time history of A3 signal of FXISO and ISODRY cases of zone III excitation

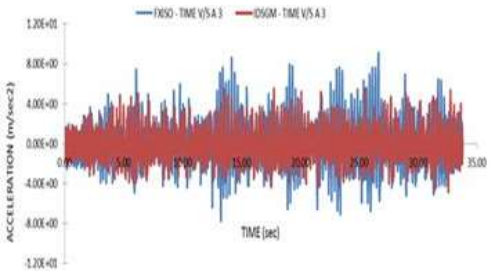

Fig. 4(b) Acceleration time history of A3 signal of FXISO and IDSGM cases of zone III excitation

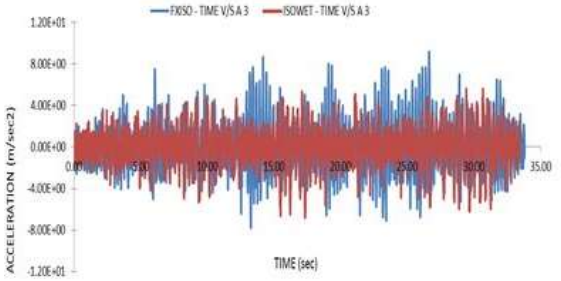

Fig. 4(c) Acceleration time history of A3 signal of FXISO and ISOWET cases of zone III excitation

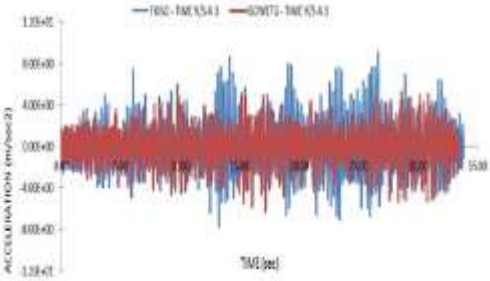

Fig. 4(d) Acceleration time history of A3 signal for FXISO and ISOWETG cases of zone III excitation

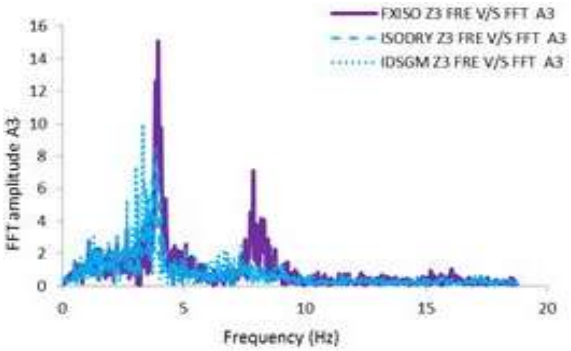

Fig. 5(a) Fourier spectra along X direction

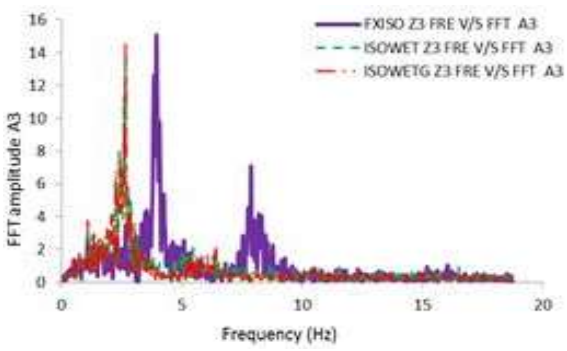

Fig. 5(b) Fourier spectra along X direction

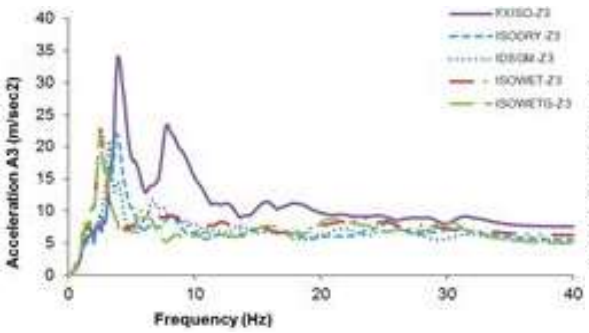

Fig. 6 Response spectra generated from acceleration time history recorded by accelerometer A3 along X direction for zone III excitation

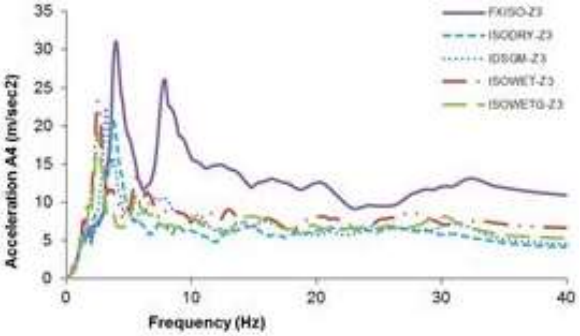

Fig. 7 Response spectra generated from acceleration time history recorded by accelerometer A4 along Y direction for zone III excitation

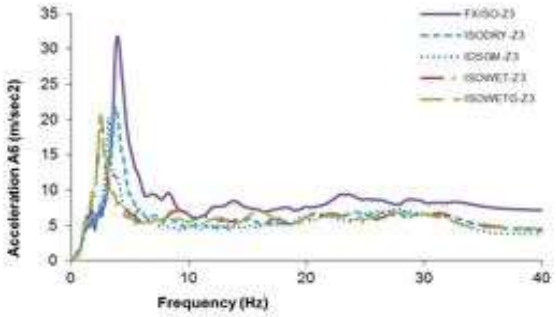

Fig. 8 Response spectra generated from acceleration time history recorded by accelerometer A6 along X direction for zone III excitation

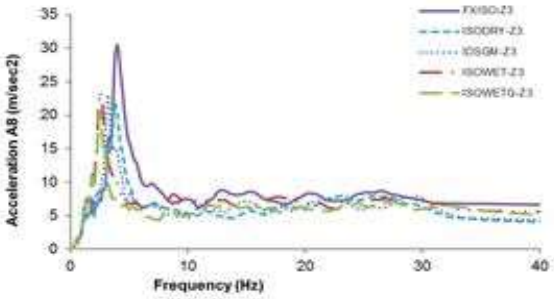

Fig. 9 Response spectra generated from acceleration time history recorded by accelerometer A8 along Y direction for zone III excitation

5. Test for IS - 1893 zone V design basis ground motion

Artificial acceleration time history, compatible to zone V of IS-1893 code, is given in Fig. 3(b), which is used in testing of the isolated footing model. Table 5 shows maximum accelerations recorded at roof level of the model in different cases. It is seen from the table that, there is a general reduction in accelerations along horizontal direction at roof level in the range of 20.41% for ISOWET case to 60.63% for RDSGM case. This reduction is more than that in the case of Zone III. From this it can be inferred that the isolation effect increases with increased amplitudes of excitation. However, like in zone III, here also it is observed that there is an increase in accelerations in vertical direction. This is due to the rigid frequency of 65.61 Hz has reduced to the zone of amplification e.g., 10.93 Hz in the case of ISODRY.

Acceleration recorded along X direction are compared in all the cases and are shown in Figs. 10(a) to 10(d). It can be seen that the peak accelerations recorded are less compared to the fixed base case. Further, Fourier amplitudes of the above signal are obtained and shown in Figs. 11(a) and 11(b). It can be seen that, there is a significant shift in the frequencies in all the cases.

Response spectrum for 5% damping was generated from the output signal of accelerometers

located at roof level of the model to understand the frequency contents of the signal and is shown in Figs 12 to 15 for various cases. It can be observed that there is a shift in the frequency in all the cases compared to the case of fixed base. Similar to the observations made in the case of tests with IS-1893 zone III time history, reduction in frequencies along with increased damping resulted in reducing accelerations. This conclusion verifies with above FFT analysis.

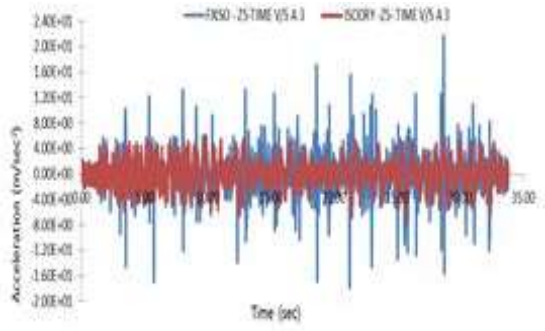

Fig. 10(a) Acceleration time history for A3 signal for FXISO and ISODRY cases of zone V excitation

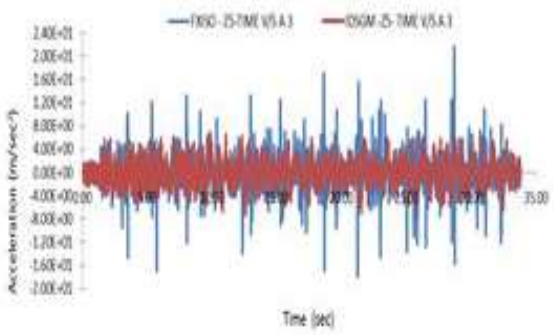

Fig. 10(b) Acceleration time history for A3 signal for FXISO and IDSGM cases of zone V excitation

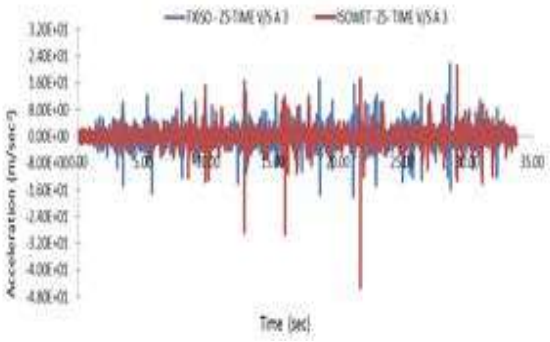

Fig. 10(c) Acceleration time history for A3 signal for FXISO and ISOWET cases of zone V excitation

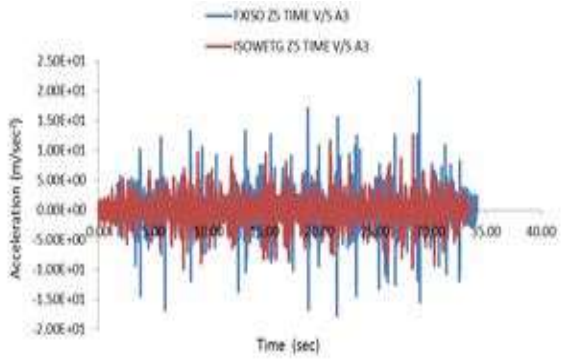

Fig. 10(d) Acceleration time history for A3 signal for FXISO and ISOWETG cases of zone V excitation

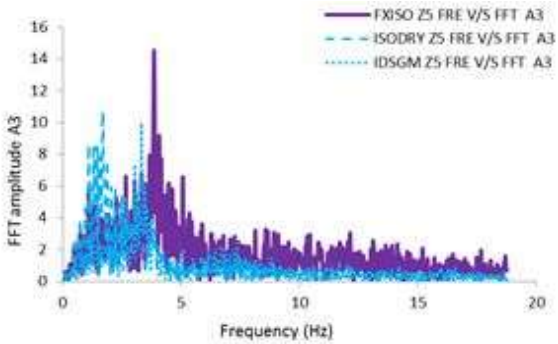

Fig. 11(a) FFT amplitudes of A3 signal of FXISO and ISODRY, IDSGM cases

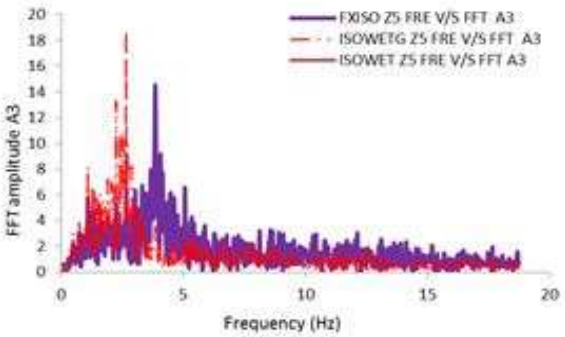

Fig. 11(b) FFT amplitudes of A3 signal of FXISO and ISOWET, ISOWETG cases

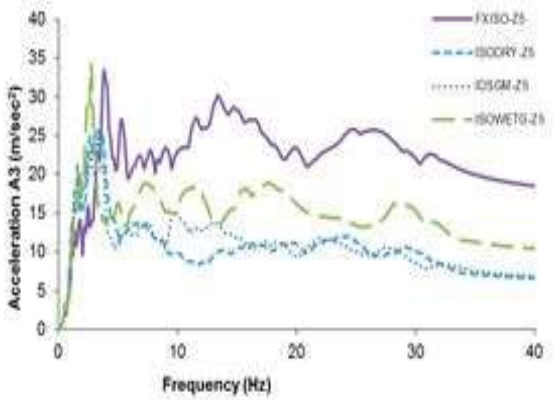

Fig. 12 Response spectra generated from acceleration time history recorded by accelerometer A3 along X direction

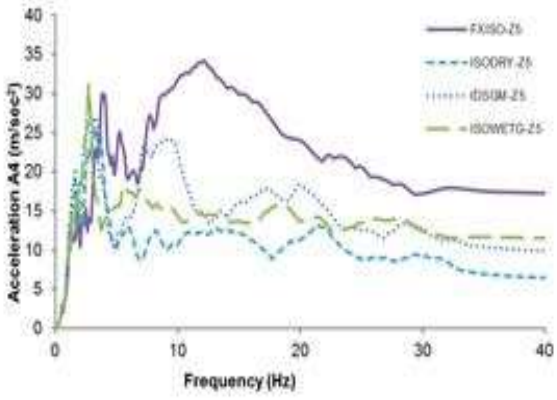

Fig. 13 Response spectra generated from acceleration time history recorded by accelerometer A4 along Y direction

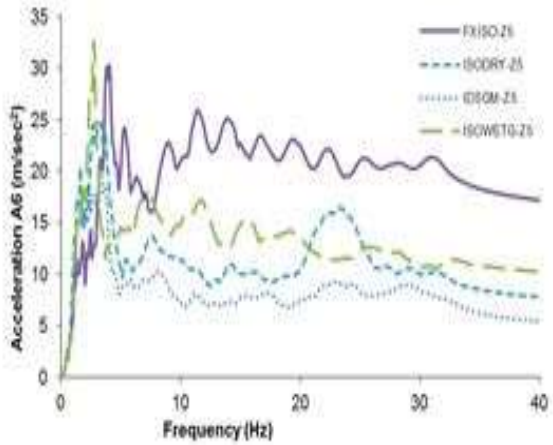

Fig. 14 Response spectra generated from acceleration time history recorded by accelerometer A6 along X direction

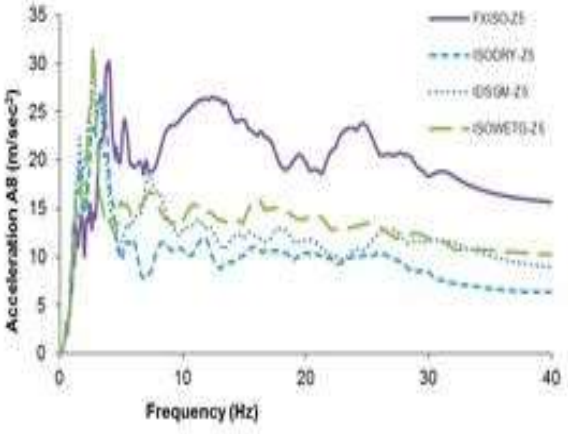

Fig. 15 Response spectra generated from acceleration time history recorded by accelerometer A8 along Y direction

6. Analysis and results

FE model of the structure is prepared using STAAD.pro software (Structural design software) and is shown in Fig. 16(a). Columns and beams are modeled in beam elements whereas roof slab and isolated footings are modeled in plate elements. In the first step, analysis was performed for spectrum compatible time histories as shown in Fig. 16(b) and Fig. 16(c). The sand layer is replaced with two horizontal and one vertical spring at four locations and properties of spring are evaluated using following procedure.

6.1 Vertical springs

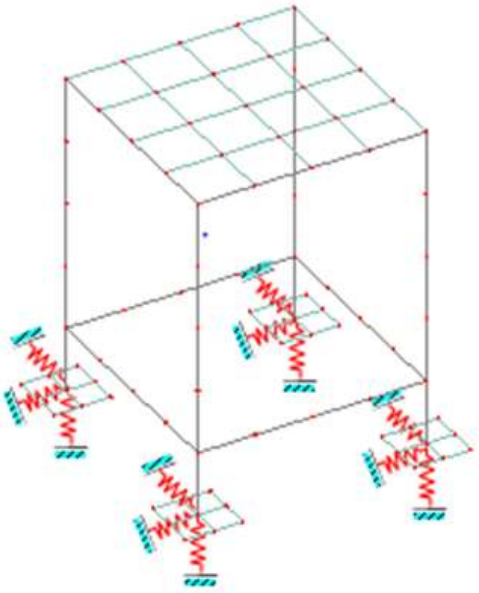

Fig. 16(a) FE mesh of RCC model with isolated footing base

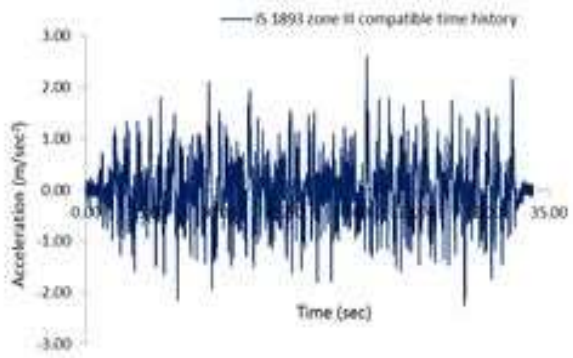

Fig. 16(b) IS 1893 zone III compatible time history

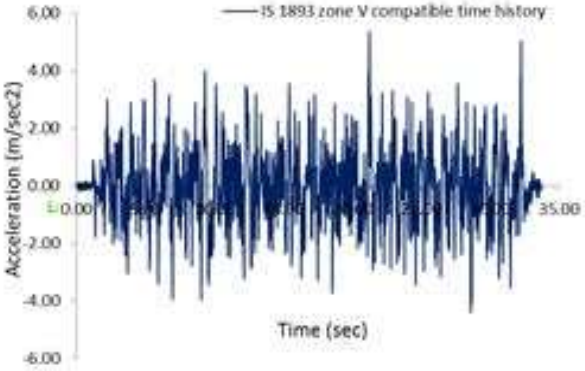

Fig. 16(c) IS 1893 zone V compatible time history

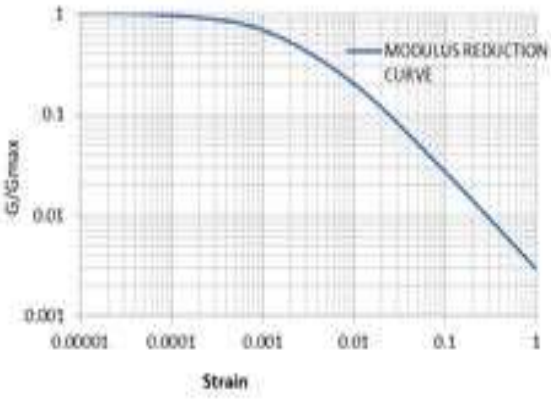

Fig. 17(a) Modulus reduction curve for sand

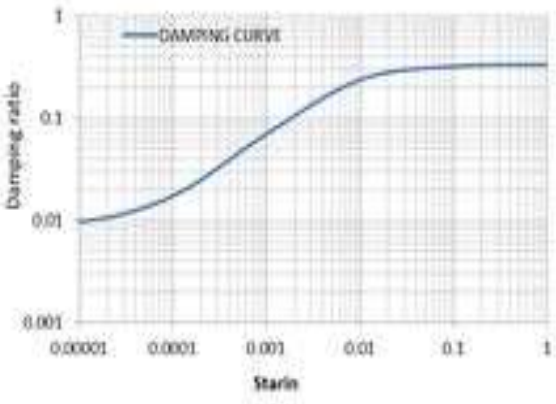

Fig. 17(b) Damping ratio curve for sand

It is well known that the shear modulus G is related with the Young's modulus E_s as follows

$$G = \frac{E_s}{2(1+\nu)} \tag{1}$$

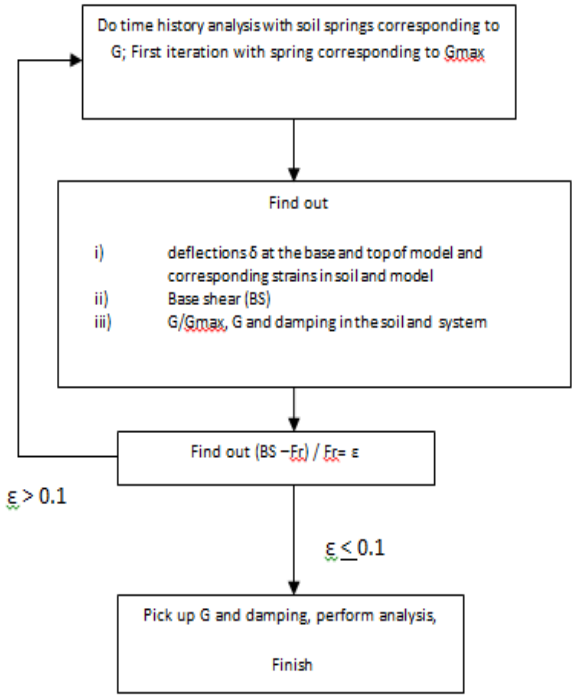

Fig. 18(a) Flow chart for iterative procedure

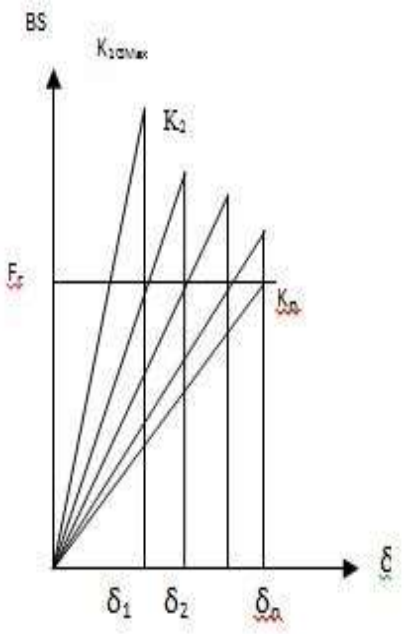

Fig. 18(b) Graphical representation of iterative procedure

where v=Poisson ratio.

The values of Young's moduli are evaluated by cyclic tri-axial tests (BRNS research report 2009) and are given as 10 MPa, 8 MPa, 6 MPa and 4 MPa respectively for ISODRY, RDSGM, ISOWET and ISOWETG cases.

The values of Poisson's ratio are taken as 0.4, 0.35, 0.4 and 0.4 for ISODRY, RDSGM, ISOWET and ISOWETG cases respectively (BRNS research report 2009, Bowels Joseph E., Arora K.R.) Knowing the value of G from Eq.1, frequency independent vertical soil spring (Kv) was calculated by following Eq. (2) (IAEA TECDOC 1347)

$$K_v = \frac{G}{(1-\nu)} \beta_\psi \sqrt{BL} \tag{2}$$

Where β_ψ is a factor to be read from the graphs (IAEA TECDOC 1347); for square footing its value are 2.15. L and B are footing length and breadth along and perpendicular to the direction of excitation respectively.

6.2 Horizontal springs

Horizontal soil spring values were calculated using iterative procedure as explained in subsequent paragraphs.

Iterative procedure to find out equivalent stiffness of soil is as given below-

To estimate the resistance offered by the sand in horizontal direction, iterative procedure (Reddy 2012) adopted is explained in the following steps.

Step 1. - Horizontal stiffness is evaluated using the following equation.

$$K = 2 \times (1 + \nu) \times G \times \beta_x \times \sqrt{B \times L} \tag{3}$$

Where v is Poisson's ratio of soil, βx is constant and is 1.0 in the present case (IAEA TECDOC 1347); L and B are footing length and breadth along and perpendicular to the direction of excitation respectively.

Using these vertical and horizontal springs; linear time history analysis is performed using spectrum compatible time histories as shown in Fig. 16(a) and 16(b) and obtained displacements, accelerations at various locations of the structure including the soil. The response displacements of horizontal spring obtained are used to calculate the shear strains developed in the soil.

Step 2. - Using plasticity index as zero for sand in ISODRY, IDSGM, ISOWET and ISOWETG cases, the shear modulus and damping characteristics is obtained and shown in Fig. 17(a) and (b).

Using these figures, reduced modulus and corresponding damping ratio is obtained corresponding to the strain calculated in step 1. Then stiffness of the soil springs are calculated with this reduced modulus. Also calculated equivalent system damping using energy principle considering the new damping of the soil along with structural damping using following Eq. (4)

$$\xi_{system} = \frac{\xi_{soil} \times W_{S\,soil} + \xi_{structure} \times W_{S_{structure}}}{4 \times \pi \times \left(W_{S_{soil}} + W_{S_{structure}}\right)} \tag{4}$$

$$\text{Where strain energy in soil} \quad Ws_{(soil)} = \frac{1}{2} \times K \times \delta^2{}_{soil} \tag{5}$$

$$\text{Strain energy in structure} \quad Ws_{(struc)} = \frac{1}{2} \times K_{struc} \times \delta^2{}_{struc} \tag{6}$$

Step 3 - Using above modified properties of the soil and equivalent system damping, time history analysis is performed and the response of the structure is obtained.

Step 4 - The above steps are repeated till the base shear is nearly equal, say within 10%, to limiting friction force *Fr*, where *Fr* is given by Eq. (7)

$$Fr = \mu \times R \tag{7}$$

Where μ=co-efficient of friction at the base of the structure.

Co-efficient of friction in case of soil is given by tanϕ, where ϕ is friction angle of soil. The friction angles measured for dry sand is 40°, dry sand with geo-membrane is 22°, wet sand is 20° and wet sand with geo-membrane is 16° (BRNS research report, 2009). The friction angle between bottom surface of concrete isolated footings and sand particles is taken as 22° (Kramer 2007)

R=reaction force on the model due to its own weight.

The model starts sliding if -

$$Fs \geq Fr \tag{8}$$

The flow chart for the iterative procedure is given in Fig. 18a and graphical representation of iterative process is given in Fig. 18(b).

In the above procedure, it is assumed that the response accelerations are governed when the structure is sticking to the soil. The displacements are governed when the structure slides on the sand bed. The displacement calculations are discussed in subsequent sections.

6.3 Analysis of the structure for zone III input

Response accelerations found out analytically and experimentally are given in table 6 for zone III excitation. Responses recorded by accelerometer A3 for ISODRY, IDSGM, ISOWET and ISOWETG cases for zone III excitation are compared with the analysis results in Figs. 19(a) to 19(d). The experimental values are observed with three direction motion applied concurrently and analytical values are found by applying one direction motion at a time. It can be seen that the analytical and experimental results have a good match.

6.4 Analysis of the structure for zone V input

Response accelerations found out analytically and experimentally are given in Table 7 for zone

Table 6 Comparison of experimental and analytical Accelerations (m/sec^2) for Zone III

Model condition / Location	FXISO		Z3-ISODRY		Z3-IDSGM		Z3-ISOWET		Z3-ISOWETG	
	Exp. Max acc	Ana. Max acc	Exp. Max acc	Ana. Max acc	Exp. Max acc	Ana. Max acc	Exp. Max acc	Ana. Max acc	Exp. Max acc	Ana. Max acc
A3	7.06	5.98	5.21	5.16	4.84	4.55	5.57	4.60	5.20	4.68
A6	7.06	5.98	5.38	5.16	4.66	4.55	4.99	4.60	5.20	4.68
A4	7.59	6.00	4.88	5.16	5.18	4.60	6.14	4.91	5.20	4.54
A8	7.29	6.00	4.79	5.16	5.45	4.60	6.24	4.91	5.30	4.54
A9	3.59	3.57	3.77	2.97	3.64	3.12	3.67	3.97	3.90	2.58

A3 along X direction at roof beam-column junction; A6 along X direction at mid span of roof beam; A4 along Y direction at roof beam-column junction; A8 along Y direction at mid span of roof beam; A9 along Z direction at center of top slab

Table 7 Comparison of experimental and analytical Accelerations (m/sec^2) for Zone V

Model condition / Accelerometer location	FXISO		Z5-ISODRY		Z5-IDSGM		Z5-ISOWET		Z5-ISOWETG	
	Exp. Max acc	Ana. Max acc	Exp. Max acc	Ana. Max acc	Exp. Max acc	Ana. Max acc	Exp. Max acc	Ana. Max acc	Exp. Max acc	Ana. Max acc
A3	14.30	12.50	7.41	9.22	6.72	9.23	10.00	9.40	9.98	9.32
A6	14.30	12.50	7.89	9.22	5.63	9.23	10.50	9.40	10.00	9.32
A4	14.70	12.40	7.23	9.05	7.21	9.13	10.50	9.46	9.77	9.14
A8	14.70	12.40	7.70	9.05	8.09	9.13	11.70	9.46	10.00	9.14
A9	8.38	7.32	6.93	4.50	6.73	4.68	6.13	4.15	7.00	4.13

A3=Dir-X, location-beam-column junction at Roof level; A6=Dir-X, location-at mid span of roof beam; A4=Dir-Y, location-beam-column junction at Roof level; A8=Dir-Y, location-at mid span of roof beam; A9=Dir-Z, location - center of slab

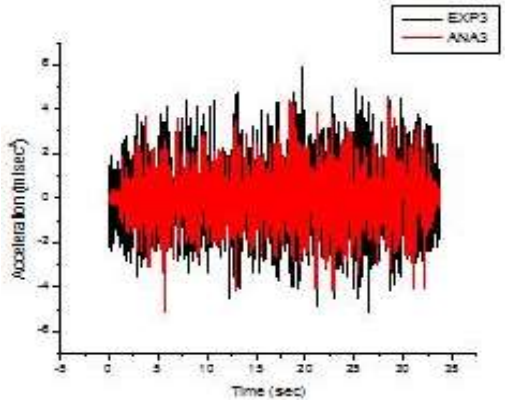

Fig. 19(a) Comparison of experimental response with analytical result of ISODRY A3 signal for zone III

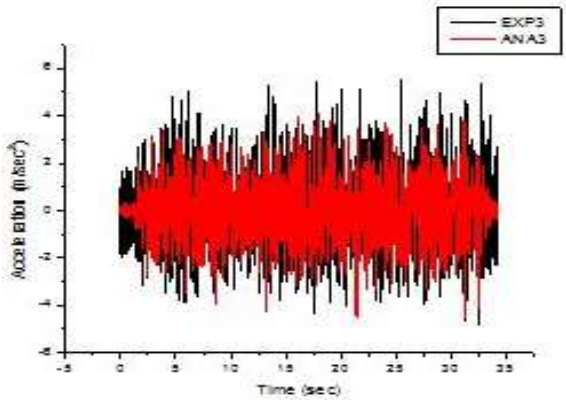

Fig. 19(b) Comparison of experimental response with analytical result of IDSGM A3 signal for zone III excitation

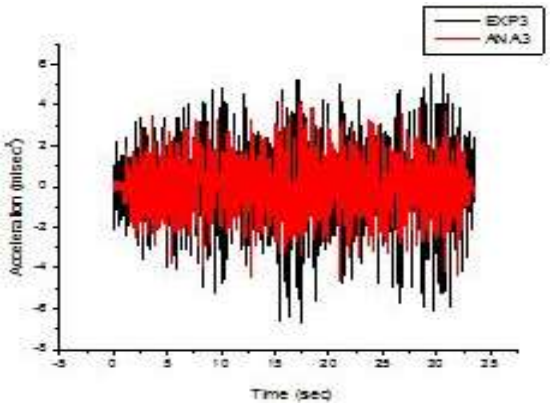

Fig. 19(c) Comparison of experimental response with analytical result of ISOWET A3 signal for zone III

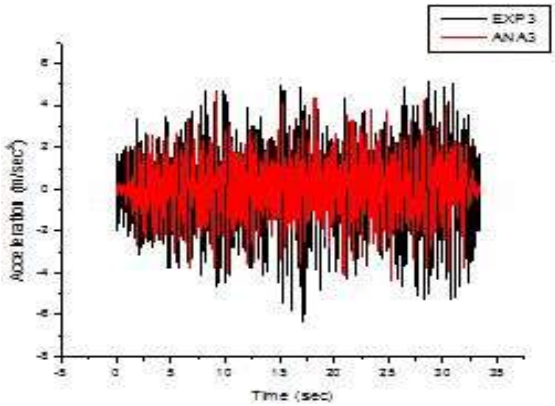

Fig. 19(d) Comparison of experimental response with analytical result of ISOWETG A3 signal for zone III

V excitation.

Responses recorded by accelerometer A3 for the cases ISODRY, RDSGM ISOWET and ISOWETG for zone V excitation are compared with the analysis results in Figs. 20(a) to 20(d). There is a good match between the analytical and experimental results.

6.5 Displacement estimation

Displacements at the bottom of the model were measured for zone III and zone V cases. The displacements found out analytically are compared with the experimental displacements in Table 8. The experimentally found displacements for zone III are on higher side. This is due to the fact that the experiments are conducted with three mutually perpendicular direction motions (X, Y horizontal and Z vertical) simultaneously and the analysis was done with one direction motion at a time. The Stiffness of the soil is sufficiently degraded due to higher deformations in case of zone V excitations and as such there is a less difference between experimental and analytical displacements.

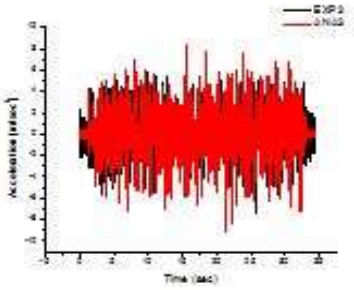

Fig. 20(a) Comparison of experimental response with analytical result of ISODRY A3 signal for zone V excitation

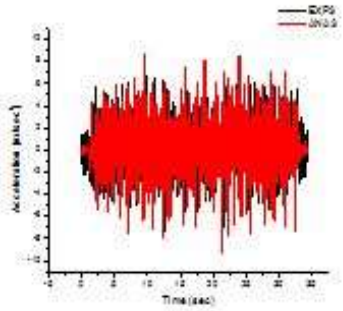

Fig. 20(b) Comparison of experimental response with analytical result of IDSGM A3 signal for zone V excitation

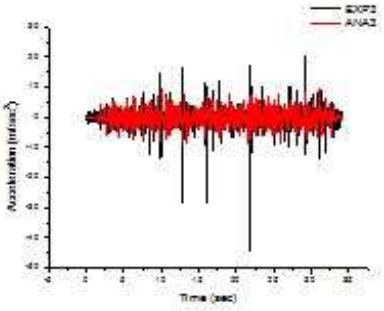

Fig. 20(c) Comparison of experimental response with analytical result of ISOWET A3 signal for zone V excitation

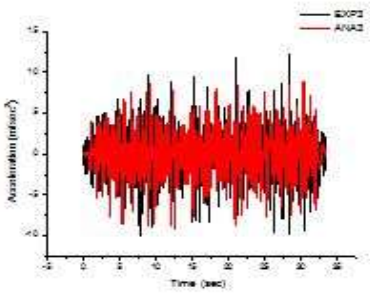

Fig. 20(d) Comparison of experimental response with analytical result of ISOWETG A3 signal for zone V excitation

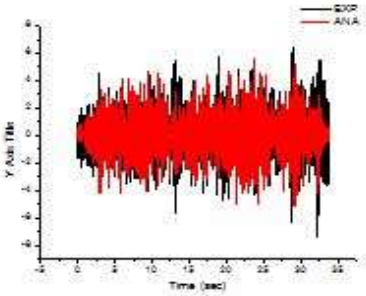

Fig. 20(e) Comparison of experimental response with analytical result of FXISO A3 signal for zone III

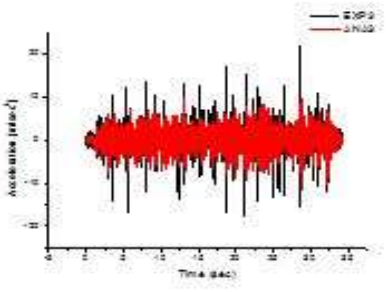

Fig. 20(f) Comparison of experimental response with analytical result of FXISO A3 signal for zone V

Table 8 Displacements of model

Model condition	Experimentally found max displacements (mm)		Analytically found max displacements (mm)	
	Zone III case	Zone V case	Zone III case	Zone V case
ISODRY	8.00	30.50	4.12	27.00
IDSGM	9.00	33.70	4.85	37.50
ISOWET	12.00	55.30	5.67	55.10
ISOWETG	20.00	54.85	18.00	69.70

Deformations of structural components were not measured separately as the accelerations at those locations are implying the extent of deformations. Also it can be seen from the above study that the accelerations at the top of the model structure placed on sand layer are reduced as compared to the one with fixed base. This implies that the deformations in the structural components too are reduced.

7. Conclusions

• Introduction of soil layer between isolated footing and hard foundation gives isolation effect to the structure. The degree of isolation will vary depending on the soil properties and magnitude of ground motion. Lower the friction coefficient, greater is the isolation effect and more the magnitude of ground acceleration, more will be the isolation effect.

• Sand layer acts as a soft layer between base of the structure and hard foundations. During earthquake excitation, the structure acts as a non-sliding structure till base shear achieves the value equal to limiting friction force. When base shear exceeds the value of limiting friction force, the structure starts sliding on the sand layer. Due to sliding motion of the structure, the part of energy of earth quake excitation gets dissipated in the sand layer and remaining energy reaches to the structure.

• The friction force is governed by vertical component of ground motion and thereby vertical motion of the structure.

• Frequency of the structure decreases with increase in excitation force and for zone V motion it attains even lower than 2 Hz; thereby indicating a good isolation of the structure. Frequency also reduces with reduction in friction coefficient.

• It is observed that the damping ratio of the structure on sand layer increases due to sliding of the structure; and thus a good amount of the excitation energy is dissipated in friction. Thus structure experiences lesser accelerations as compared to fixed base structure.

• The motion of the structure is divided in to two phases viz. non-sliding (sticking) phase and sliding phase. The maximum acceleration is experienced by the structure during non-sliding phase and maximum displacement during sliding phase. From the FFT analysis, it is seen that there are more than one distinct peaks of different amplification as the structure experiences major amplification of acceleration in non-sliding phase and lower amplification in acceleration during sliding phase.

• During the sliding of the structure, it is displaced from the original position. However, due to mean zero characteristics of ground motion, the position of the structure will not change significantly.

• Thickness of sand layer tried was 300 mm in the experimental set up. Effect of variation in thickness of sand layer on the base isolation characteristics can be studied.

• Average percentage reduction in horizontal accelerations achieved are 30, 31, 21, 28 for ISODRY, IDSGM, ISOWET, ISOWETG cases respectively for zone III and 48, 52, 26, 31 for ISODRY, IDSGM, ISOWET, ISOWETG cases respectively for zone V excitation by interposing of sand layer below the structure. The isolation effect is highest in IDSGM case and then in ISODRY, ISOWETG and ISOWET cases in decreasing order.

• Sand layer provided for isolation effect in practical applications may get wet due to possible ingress of ground water into the layer. The effect is studied by taking wet sand layer cases e.g., ISOWET, ISOWETG. It is found that there is no liquefaction occurred.

• The bearing capacity of foundation soil remains unaltered in case of structures provided with natural seismic base isolation.

• Sand is a natural material and is physically and chemically stable against all the forces and chemical agents normally expected to encounter during life time of the structure. Hence change in its inherent properties during life time is negligible. As such uncertainty involved in its functioning during life time is negligible. It does not require any maintenance. Hence it is more reliable

• The technique can be adopted to any type of structure including Nuclear Power Plant (NPP) structures. But looking to the importance of NPPs and the size of model tested, one need to go for more tests on larger size models

Acknowledgements

Authors are grateful to Heavy Water Board, Bhabha Atomic Research Center, National Institute of Technology, Suratkal and Central Power Research Institute, India for promoting and supporting the present research work.

References

Arora, K.R. (1992), *Soil Mechanics And Foundation Engineering*, IIIrd edition, Standard publishers and distributers, New Delhi, India.

Bowels, Joseph E. (1977), *Foundation Analysis and Design*, 2nd edition, Mc Graw-Hill, New York, USA.

BRNS research report (2009), "Dynamic soil structure interaction effects in multistoried structures on homogeneous soil and geo-synthetic reinforced soil", NITK, Suratkal, India.

Feng, Z.Y. and Sutter, K.G. (2000), "Dynamic properties of rubber sand mixtures", *Geotech. Test. J.*, **23**(3), 338-344.

Foose, G.J. and Benson, C.H. (1996), "Sand reinforced with shredded waste tires", *Geotech. Geoenvir. Eng*., **122**(9), 760-767.

IAEA TECDOC 1347 (2003), *Consideration Of External Events In The Design Of Nuclear Facilities Other Than Nuclear Power Plants, With Emphasis On Earthquakes*.

IS 1893 (2002), *Criteria for earthquake resistant design of structures (part 1 general provisions and buildings)*, Bureau of Indian Standards, New Delhi, India

Ivan, Skinner R., William, H. Robinson and Graeme, H. Mcverry (1996), *An Introduction to Seismic Isolation*, Wiley, New York, USA

Jangid, R.S. (1996), "Seismic response of sliding structures to bidirectional earthquake excitation", *Earthq. Eng. Struct. Dyn*., **25**(11), 1301-1306.

Jangid, R.S. and Datta, T.K. (1995), "Seismic behavior of base isolated buildings: a-state of the art review", *Struct. Build.*, **110**(2), 186-203.

Karabork, T., I.O., Deneme and R.P., Bilgehan (2014), "A comparision of the SSI on base isolated systems and fixed base structures for soft soil", *Geomech. Eng*., **7**(1), 87-103.

Kramer, Steven L. (2007), *Geotechnical Earthquake Engineering*, Published by Dorling Kindersley (India) Pvt. Ltd., licensees of Pearson Education in South Asia.

Massimo, Forni, Rodolfo, Antonucci, Alessandra, Arcadi and Antonio, Occhiuzzi (2004), "A hybrid seismic isolation system made of rubber bearings and semi-active magneto-rheological dampers", *13th World Conference on Earthquake Engineering*, Vancouver, B.C., Canada.

Naeim, F. and Kelly, J.M. (1999), *Design of seismic isolated structures: from theory to practice*, John Wiley & Sons, Inc, New York, USA.

Parulekar, Y.M., Reddy, G.R., Vaze, K.K. and Ghosh, A.K. (2007), "Seismic response control of complex piping system using elasto-plastic dampers - Experiments and analysis", *International Workshop on Earthquake Hazards & Mitigations on December 7-8, 2007 at IIT Guwahati*, India.

Parulekar, Y.M., Reddy, G.R., Vaze, K.K., Ghosh, A.K., Khushavha, H.S., Muthumani, K. and Sreekala (2004), "Passive seismic control of piping system using shape memory alloy damper", *13th Symposium on Earthquake Engineering held at IIT*, Roorkee.

Peter, J.B. and Tuncer, B.E. (1994), "Engineering properties of tire chips and soil mixtures", *Geotech. Test. J*., **17**(4), 453-464.

Reddy, G.R. (2012), "Response spectrum method for non-linear systems", *Proceedings of fourth International Conference on structural stability and dynamics*.

Satish, Kumar, K., Muthumani, N., Gopalkrishnan and R., Sreekala (2004), "Design scheme for seismic retrofitting of structures using visco-elastic damper devices", *13th Symposium on Earthquake Engineering held at IIT*, Roorkee.

Srijit, Bandopsdhyay and Aniruddha, Sengupta (2012), "Experimental investigation into natural base isolation system for earthquake protection", M. Tech thesis of IIT, Kharagpur, India.
STAAD, Pro 2006.
Tsang, H.H. (2008), "Seismic isolation by rubber soil mixtures for developing countries", *Earthq. Eng. Struct. Dyn*., **37**(2), 283-303.
Tsang, H.H., Lo, S.H., Cu, X. and Sheikh, M.N. (2012), "Seismic isolation for low-to-medium-rise buildings using granulated rubber-soil mixtures: Numerical study", *Earthq. Eng. Struct. Dyn*., **41**(14), 2009-2024.
Yegian, M.K. and Kadakal, U. (2004), "Soil isolation for seismic protection using a smooth synthetic liner", *J. Geotech. Geo-envir. Eng*., ASCE, **130**(11), 1131-1139.
Yegian, M.K. and M., Catan (2004), "Foundation isolation for seismic protection using a smooth synthetic liner", *J. Geotech. Geo-envir. Eng*., ASCE, **130**(11), 1121-1130.
Zhou, F.L., Yang, Z., Liu, W.G. and Tan, P. (2004), "New seismic isolation system for irregular structure with the largest isolaton building area in the world", *13th World Conference on Earthquake Engineering*, Vancouver, B.C., Canada.

CC